

## Dependence of the flux-creep time scale on sample size for melt-textured $\text{YBa}_2\text{Cu}_3\text{O}_7$ by ac-susceptibility measurements

C. Ren and S. Y. Ding

*Department of Physics and National Laboratory of Solid State Microstructures, Center for Advanced Studies in Science and Technology of Microstructures, Nanjing University, Nanjing, 210008, People's Republic of China*

Z. Y. Zheng

*Department of Physics and National Laboratory of Solid State Microstructures, Center for Advanced Studies in Science and Technology of Microstructures, Nanjing University, Nanjing, 210008, People's Republic of China*  
and *Department of Physics, Engineering Institute for Engineer Corps, Nanjing, 210007, People's Republic of China*

M. J. Qin and X. X. Yao

*Department of Physics and National Laboratory of Solid State Microstructures, Center for Advanced Studies in Science and Technology of Microstructures, Nanjing University, Nanjing, 210008, People's Republic of China*

Y. X. Fu and C. B. Cai

*Shanghai Institute of Metallurgy, Academia Sinica, Shanghai 20050, People's Republic of China*

(Received 31 July 1995)

The complex ac susceptibility  $\chi$  was measured as a function of temperature  $T$ , ac field frequency  $f$ , and amplitude  $H_{ac}$  for three textured  $\text{YBa}_2\text{Cu}_3\text{O}_7$  samples with different sizes  $d$ . The effects of  $f$  and  $H_{ac}$  on the peak temperature  $T_p$  in  $\chi''$  were analyzed based on nonlinear flux diffusion theory. The current-density- ( $j$ -) dependent effective activation barriers  $U(j) \propto \ln(j_0/j)$  have been extracted in a time window of milliseconds and are the same as those obtained in other time windows. Flux-creep time scales  $t_0$  of  $10^{-5}$  and  $10^{-7}$  s have been extracted for the large ( $d \approx 1$  mm) and small ( $d \approx 10$   $\mu\text{m}$ ) samples, respectively. The fact that  $t_0$  increases with sample size shows that it is a macroscopic quantity, as predicted by the nonlinear flux diffusion theory.

The flux-creep of high- $T_c$  superconductors (HTS's) have been widely discussed<sup>1</sup> and the flux-creep time scale  $t_0$  appearing in a variety of flux-creep equations is often considered to be a microscopic time scale somehow related to vortex hopping.<sup>2</sup> Recently, theory has predicted that  $t_0$  is a macroscopic quantity dependent on external field, current density, and sample size, etc., as observed in experiments.<sup>1,3</sup>

The susceptibility (ACS) technique has been widely used to study magnetic properties for various materials.<sup>4,5</sup> We have determined  $t_0$ 's for  $\text{TlBa}_2\text{Ca}_2\text{Cu}_3\text{O}_x$  (TI-1223) and  $\text{HgBa}_2\text{Ca}_2\text{Cu}_3\text{O}_y$  (Hg-1223) HTS's by this technique.<sup>6,7</sup> In this paper, we report the determination of  $t_0$  and the effective activation energy by ACS experiments  $U(j)$  for three textured  $\text{YBa}_2\text{Cu}_3\text{O}_7$  (YBCO) samples with different sizes and show how  $t_0$  is related to the sample size.

Three slab YBCO samples 1, 2, and 3 were grown by melt-textured growth processing. X-ray diffraction pattern examinations show that they are highly  $c$ -axis textured with different effective sizes as listed in Table I. Details of sample preparation and characterization have been reported elsewhere.<sup>8,9</sup>

The ac field  $H(t) = H_d + H_{ac} \cos(2\pi ft)$  is applied with  $H_d$  and  $H_{ac}$  oriented in the  $c$ -axis direction. The temperature dependences of the real and imaginary parts of the ACS for these samples,  $\chi'(T)$  and  $\chi''(T)$ , were measured as a function of ac field frequency and amplitude in a dc field on a homemade susceptometer with sensitivity of  $10^{-8}$  emu. All data for  $\chi(T)$  were recorded by a computer for later analysis. Details of the ACS measurement and the data analysis procedure can be found in Ref. 6.

Shown in Fig. 1 are typical  $\chi''(T)$  curves at different frequencies  $f$  for sample 1, showing that the temperature at which  $\chi''$  peaks,  $T_p$ , increases with increasing frequencies. Another example, indicating that  $T_p$  decreases with increasing ac field amplitude  $H_{ac}$ , is illustrated in Fig. 2. This  $\chi''$  peak temperature dependence on  $f$  and  $H_{ac}$ ,  $T_p(f, H_{ac})$ , was also observed for samples 2 and 3 but is not shown here. We explain the mechanism underlying these  $\chi''$  peaks as nonlinear thermal-activated flux diffusion, that is, vortices or vortex bundles diffuse over a nonlinear barrier  $U$ . There are other mechanisms which can also lead to a  $\chi''$  peak.<sup>10-12</sup> For example, if the ACS is caused by a static flux-pinning effect,  $T_p$  depends only on  $H_{ac}$ , whereas if  $T_p$  depends only on  $f$  the linear resistivity of flux motion accounts for the ac susceptibility. However, neither of these mechanisms can account for the present  $\chi(T)$  data.

The nonlinear flux diffusion theory predicts that  $T_p$  depends on both  $f$  and  $H_{ac}$ .<sup>1,10</sup> Considering a thin slab with thickness  $2d$  along the  $x$  axis in an applied ac field  $H(t)$ , we

TABLE I.  $t_0$  at  $H_{ac}=2.9$  G and  $H_d=2000$  G for YBCO samples 1-3, TI-1223 (Ref. 6) and Hg-1223 (Ref. 7).

	1	2	3	TI-1223	Hg-1223
$d$ (mm)	1.2	0.9	0.013	0.005	0.001
$T_x$ (K)	89.8	91	87	117	117
$U_0$ (eV)	1.37	1.24	0.64	9.8	1.06
$t_0$ ( $10^{-5}$ s)	2.7	2.5	0.05	0.01	0.005

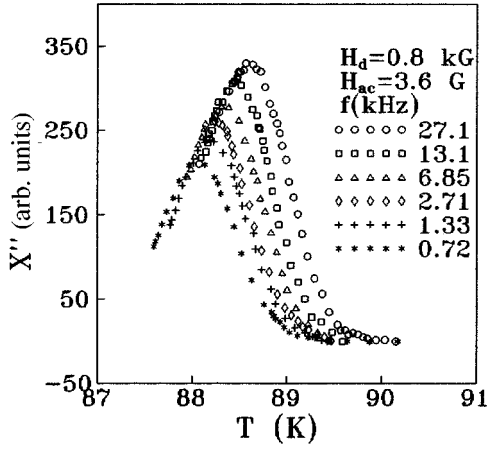


FIG. 1. Typical  $\chi''(T)$  curves at five frequencies  $f$  for sample 1, showing the peak temperature  $T_p$  shifted by the operating frequency.

have the continuity equation of indication  $B$

$$\partial_t B + \partial_x (Bv) = 0. \quad (1)$$

Supposing that the velocity of flux lines obeys the Arrhenius law  $v = v_0 e^{-U/T}$  and solving Eq. (1) perturbatively to logarithmic accuracy, Blatter *et al.* obtained the criteria for the peak in  $\chi''$  of the ACS:<sup>1</sup>

$$U(T_p, H_d, j) = T_p \ln[1 + 1/(ft_0)], \quad (2a)$$

$$j(T_p, H_d, f) = H_{ac}/d, \quad (2b)$$

$$t_0 = T_p d^2 / (2H_d v_0 |\partial_j U|), \quad (2c)$$

where  $t_0$  is a time scale,  $j$  is the current density, and  $1/f = t$  is the relaxation time during which the moment (current) of the sample has been relaxing ( $t=0$  is the critical state). Equations (2) indicate that  $T_p(f, H_{ac}) \{= U/\ln[1 + 1/(ft_0)]\}$  data can be used to determine the relaxation time scale  $t_0$  and the activation barrier  $U$ . All of our  $T_p(f, H_{ac})$  data are summarized in Figs. 3(a)–3(c) by plotting  $\ln[1 + 1/(ft_0)]$  vs

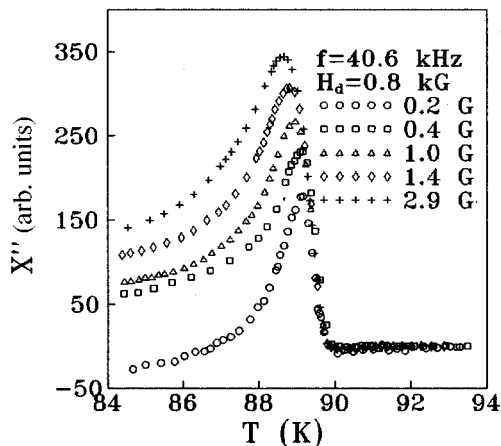
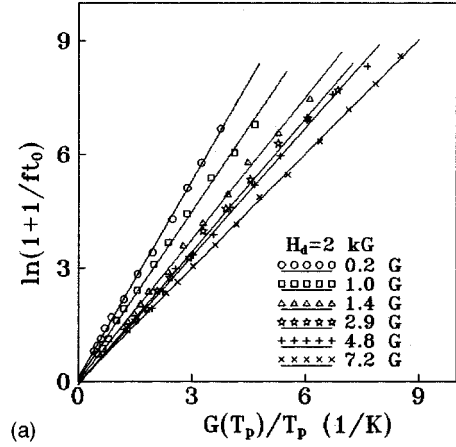
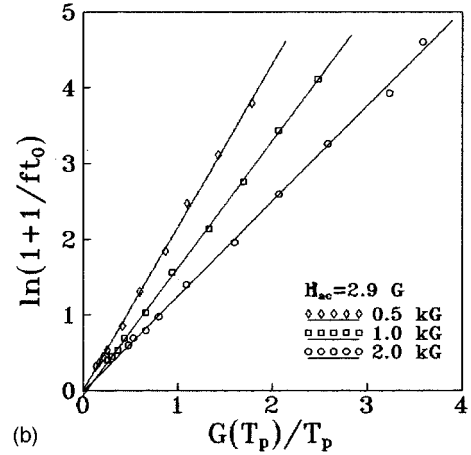


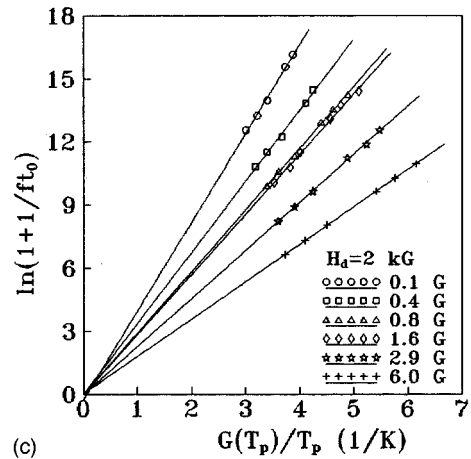
FIG. 2. Typical  $\chi''(T)$  curves at six ac field amplitudes  $H_{ac}$  for sample 1, showing the peak temperature  $T_p$  shifted by ac field amplitude  $H_{ac}$ .



(a)



(b)



(c)

FIG. 3. Data summary: The frequency- and ac-field-amplitude-dependent peak temperature in  $\chi''(T)$  curves,  $T_p(f, H_{ac})$ , data are plotted as  $\ln(1 + 1/ft_0)$  vs  $G(T_p)/T_p$  at six  $H_{ac}$  values for the three samples, where  $G(T_p) = [1 - (T_p/T_x)^2]^{3/2}$  is the temperature scaling function accounting for the temperature dependence of  $U(j, H_d, T_p) [\equiv U(j, H_d, T_p = 0 \text{ K})G(T_p)]$ , see text. The symbols are the data while the solid straight lines are fitted curves. (a) sample 1, (b) sample 2, and (c) sample 3.

$G(T_p)/T_p$  for the three samples, where  $G(T_p)$  is the temperature scaling function accounting for the temperature dependence of the barriers  $U$ , i.e.,  $U(j, H_d, T_p) \equiv U(j, H_d, T_p = 0 \text{ K})G(T_p)$ .<sup>13</sup> When we take the fitting  $G(T_p) = [1 - (T_p/T_x)^2]^{3/2}$  with  $T_x$  listed in Table I, and plot

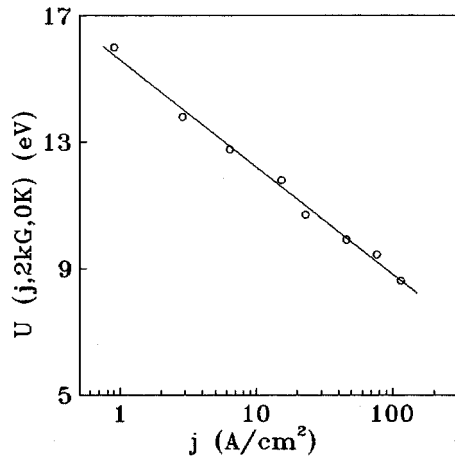


FIG. 4. One of the  $U(j)$  relationships for sample 1. The symbols are the slopes of the straight lines in Fig. 3 and the solid lines are the fitted curves described by Eq. (4).

the  $T_p(f)$  data as  $\ln(1+1/ft_0)$  vs  $G(T_p)/T_p$ , nice straight lines are obtained; see Fig. 3. It is clear that the  $t_0$  can be determined as experimental fitting parameters. The average values of  $t_0$  are also listed in Table I for the samples. It is found that the larger the sample size, the larger  $t_0$ .

Furthermore, we can explore the  $U(j)$  relationship. It is obvious that the slopes of these fitted straight lines in Fig. 3 are just the activation barriers  $U(H_{ac}, H_d, 0 \text{ K})$ . Plotting those slopes vs  $H_{ac}$  and using Eq. (2b) and  $d$  in Table I, we construct the current dependence of the activation barrier  $U(j, H_d, 0 \text{ K})$  for the samples, which depend on current density logarithmically:

$$U(j, 2 \text{ kG}, 0 \text{ K}) = U_0 \ln(j_0/j). \quad (3)$$

For example, the  $U(j)$  relation for sample 1 is shown in Fig. 4. The experimental parameters are  $U_0 = 1.37 \text{ eV}$ ,  $j_0 = 7.08 \times 10^4 \text{ A/cm}^2$  and  $U_0 = 0.64 \text{ eV}$ ,  $j_0 = 2.92 \times 10^4 \text{ A/cm}^2$  for samples 1 and 3, respectively. This kind of logarithmic  $U(j)$  function has already been reported for YBCO from transport and dc magnetic relaxation measurements.<sup>14,15</sup> It is noticed, however, that we have determined the magnetic relaxation  $j(t, T)$ , i.e.,  $H_{ac}(f, T_p)$ , because we have measured  $T_p(f, H_{ac})$ . Thus these  $U(j)$  and  $t_0$  values obtained by the ACS measurements ( $10^{-1} < f < 10^5 \text{ Hz}$ ) are in a time window of submilliseconds ( $10^{-1} > t > 10^{-5} \text{ s}$ ), whereas the dc magnetic relaxation and transport measurements usually work in the time windows of hours ( $t > 10 \text{ s}$ ) and less than microseconds ( $t < 10^{-6} \text{ s}$ ), respectively.

Because the operating frequency in this experiment is as high as 60 kHz while  $1/t_0$  is around 30 kHz,  $t_0 \ll t$  is not always correct and the constant 1 in Eq. (2a) cannot be neglected as in e.g., Refs. 1 and 10. In order to see what might happen at  $t \approx t_0$ , we represent the  $T_p(f, H_{ac})$  data by plotting  $\ln(1/f)$  vs  $G(T_p)/T_p$  in Fig. 5. It is found that the curves  $\ln(1/f)$  vs  $G(T_p)/T_p$  are still straight lines as long as  $ft_0 \gg 1$ . Nevertheless, deviations from this linearity take place at operating frequencies  $f$  comparable with the sample creep time scales  $1/t_0$ , i.e.,  $\ln(1/f)$  about  $-9.5$  ( $1/t_0 \approx 3 \times 10^4 \text{ Hz}$ ) for samples 1 and 2 [see Figs. 3(a) and 3(b)] whose sizes are larger. Meanwhile, no such deviation from linearity is found

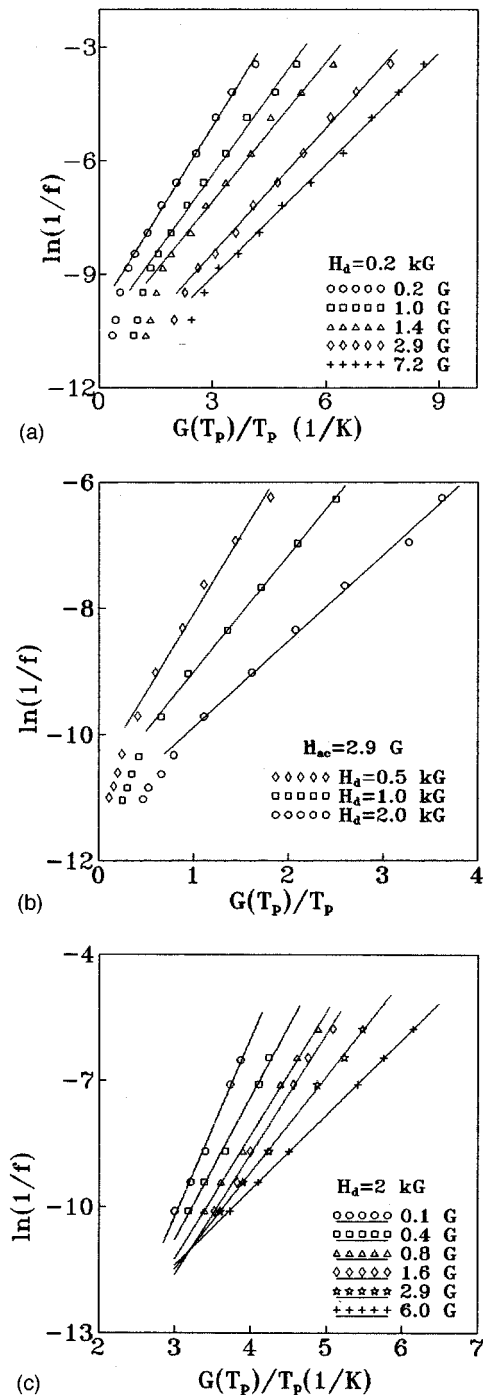


FIG. 5. Data  $T_p(f, H_{ac})$  represented by plotting  $\ln(1/f)$  vs  $G(T_p)/T_p$ , showing the positions where  $f \approx 1/t_0$  and thus  $1+1/ft_0$  cannot be written as  $1/ft_0$ . The data are taken from Fig. 3 at six ac field amplitudes. The solid lines are drawn to guide the eye. (a) Sample 1, (b) sample 2, and (c) sample 3.

for sample 3 [see Fig. 3(c)] whose size  $d$ , and thus its  $t_0$  is the smallest, leading to  $ft_0 \ll 1$  for all operating frequencies. This is a strong confirmation that  $t_0$  depends on the sample size, and the ACS technique is particularly powerful in studying the magnetic relaxation time scale.

Finally, to determine if the nonlinear theory can quantitatively describe the dependence of  $t_0$  on the sample size  $d$ , we combine Eqs. (2c), (3), and (2b) and obtain

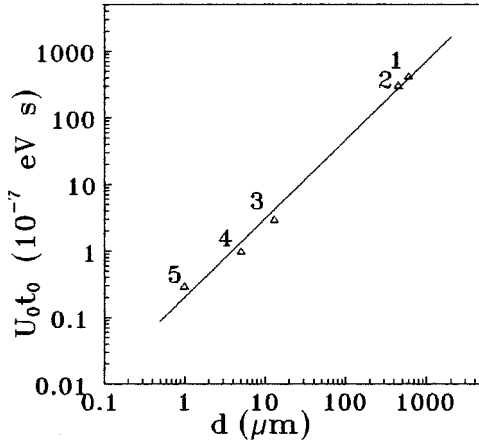


FIG. 6.  $U_0 t_0$  vs  $d$ , showing the effect of sample size  $d$  on the creep time scale  $t_0$ . 1, YBCO sample 1; 2, YBCO sample 2; 3, YBCO sample 3; 4, TI-1223; 5, Hg-1223.

$$t_0 \propto d H_{ac} / (H_d v_0 U_0) \quad (4)$$

which means that  $U_0 t_0$  is proportional to the same size  $d$  at fixed  $H_{ac}$  and  $H_d$ . Shown in Fig. 6 are the data for the

present three YBCO samples and TI-1223 (Ref. 6) and Hg-1223.<sup>7</sup> We can see that  $U_0 t_0$  is roughly proportional to the sample size. This is strong evidence showing that the flux-creep time scale  $t_0$  is a geometry-dependent parameter. The physical meaning of  $t_0$  is just as pointed out by Blatter *et al.*: the magnetization is proportional to sample volume whereas the decay of magnetization is proportional to sample surface and thus  $t_0$  is proportional to the sample size.<sup>1</sup>

In summary, we have studied flux-creep processes and flux-creep time scales  $t_0$ , as well as the diffusion activation barriers  $U(j)$ , for textured YBCO samples by means of ACS measurements.  $U(j) \propto \ln(j_0/j)$  determined in the time window ( $10^{-2} \leq t \leq 10^{-5}$  s) is the same as that observed in other windows by dc magnetic ( $t \leq 10^1$  s) and transport measurements ( $t \leq 10^{-6}$  s) in single-crystal and thin-film YBCO samples. The flux-creep time scale  $t_0$  has been shown to be  $10^{-7}$  and  $10^{-5}$  s for samples with effective sizes of the order of  $10^{-5}$  and  $10^{-3}$  m, respectively. This sample-size dependence  $t_0$  is of strong confirmation that it is a macroscopic quantity.

The authors thank L. Qiu and Professor Z. Yu for their technical help. This work was supported by the National Center for R&D on Superconductivity under Contract No. J-A-4102.

<sup>1</sup>G. Blatter, M. V. Feigel'man, V. B. Geshkenbin, A. I. Larkin, and V. M. Vinokur, *Rev. Mod. Phys.* **66**, 1125 (1994).

<sup>2</sup>P. W. Anderson and Y. B. Kim, *Rev. Mod. Phys.* **36**, 39 (1964).

<sup>3</sup>A. Gurevich and H. Kupfer, *Phys. Rev. B* **48**, 6477 (1993); *Phys. Rev. Lett.* **73**, 178 (1994).

<sup>4</sup>A. M. Campbell, *J. Phys. C* **2**, 1492 (1969).

<sup>5</sup>*Magnetic Susceptibility of Superconductors and Other Spin Systems*, edited by R. A. Hein, T. L. Francavilla, and H. D. Liebenberg (Plenum, New York, 1991).

<sup>6</sup>S. Y. Ding, G. Q. Wang, X. X. Yao, H. T. Peng, Q. Y. Peng, and S. H. Zhou, *Phys. Rev. B* **51**, 9017 (1995); S. Y. Ding, J. W. Lin, G. Q. Wang, C. Ren, X. X. Yao, H. T. Peng, Q. Y. Peng, and S. H. Zhou, *Physica C* **246**, 78 (1995).

<sup>7</sup>J. Li, S. Y. Ding, J. S. Zhu, H. M. Shao, and Y. N. Wang, *J. Appl. Phys.* **77**, 6398 (1995).

<sup>8</sup>Y. X. Fu, H. C. Yang, C. B. Cai, G. Y. Wang, T. S. Shi, and E. J.

McNiff, Jr., *Chin. Sci. Bull.* **39**, 454 (1994).

<sup>9</sup>G. Y. Wang, T. S. Shi, Y. X. Fu, C. G. Cai, and H. C. Yang, *Supercond. Sci. Technol.* **6**, 657 (1993).

<sup>10</sup>C. J. van der Beek, V. B. Geshkenbin, and V. M. Vinokur, *Phys. Rev. B* **48**, 3393 (1993).

<sup>11</sup>S. Samarappuli, A. Schiling, M. A. Chernikov, and H. R. Ott, *Physica C* **201**, 159 (1992).

<sup>12</sup>J. Giapintzakis, R. L. Neiman, D. M. Ginsberg, and M. A. Kirk, *Phys. Rev. B* **50**, 16 001 (1994).

<sup>13</sup>M. E. McHenry, S. Simizu, H. Lessure, M. D. Maley, Y. Coulters, I. Tanaka, and H. Kojima, *Phys. Rev. B* **44**, 7641 (1991).

<sup>14</sup>E. Zeldov, N. M. Amer, G. Koren, A. Gupta, and M. W. Mcelfresh, *Appl. Phys. Lett.* **56**, 680 (1990).

<sup>15</sup>M. D. Maley, J. Q. Wills, H. Lessure, and M. E. McHenry, *Phys. Rev. B* **42**, 2639 (1990).